# Interdomain Interactions within Ryanodine Receptors Regulate $Ca^{2+}$ Spark Frequency in Skeletal Muscle

Alexander Shtifman,[1] Christopher W. Ward,[1] Takeshi Yamamoto,[2] Jianli Wang,[3] Beth Olbinski,[3] Hector H. Valdivia,[3] Noriaki Ikemoto,[2] and Martin F. Schneider[1]

[1]University of Maryland School of Medicine, Department of Biochemistry and Molecular Biology, Baltimore, MD 21201
[2]Boston Biomedical Research Institute, Department of Muscle Research, Watertown, MA 02472
[3]University of Wisconsin School of Medicine, Department of Physiology, Madison, WI 53706

ABSTRACT DP4 is a 36-residue synthetic peptide that corresponds to the $Leu^{2442}$-$Pro^{2477}$ region of RyR1 that contains the reported malignant hyperthermia (MH) mutation site. It has been proposed that DP4 disrupts the normal interdomain interactions that stabilize the closed state of the $Ca^{2+}$ release channel (Yamamoto, T., R. El-Hayek, and N. Ikemoto. 2000. *J. Biol. Chem.* 275:11618–11625). We have investigated the effects of DP4 on local SR $Ca^{2+}$ release events ($Ca^{2+}$ sparks) in saponin-permeabilized frog skeletal muscle fibers using laser scanning confocal microscopy (line-scan mode, 2 ms/line), as well as the effects of DP4 on frog SR vesicles and frog single RyR $Ca^{2+}$ release channels reconstituted in planar lipid bilayers. DP4 caused a significant increase in $Ca^{2+}$ spark frequency in muscle fibers. However, the mean values of the amplitude, rise time, spatial half width, and temporal half duration of the $Ca^{2+}$ sparks, as well as the distribution of these parameters, remained essentially unchanged in the presence of DP4. Thus, DP4 increased the opening rate, but not the open time of the RyR $Ca^{2+}$ release channel(s) generating the sparks. DP4 also increased [$^3$H]ryanodine binding to SR vesicles isolated from frog and mammalian skeletal muscle, and increased the open probability of frog RyR $Ca^{2+}$ release channels reconstituted in bilayers, without changing the amplitude of the current through those channels. However, unlike in $Ca^{2+}$ spark experiments, DP4 produced a pronounced increase in the open time of channels in bilayers. The same peptide with an $Arg^{17}$ to $Cys^{17}$ replacement (DP4mut), which corresponds to the $Arg^{2458}$-to-$Cys^{2458}$ mutation in MH, did not produce a significant effect on RyR activation in muscle fibers, bilayers, or SR vesicles. $Mg^{2+}$ dependence experiments conducted with permeabilized muscle fibers indicate that DP4 preferentially binds to partially $Mg^{2+}$-free RyR(s), thus promoting channel opening and production of $Ca^{2+}$ sparks.

KEY WORDS: E-C coupling • $Ca^{2+}$ release channel • domain peptides • $Ca^{2+}$-induced $Ca^{2+}$ release • sarcoplasmic reticulum

## INTRODUCTION

In skeletal muscle, excitation-contraction coupling is initiated by a nerve impulse that produces an action potential that rapidly propagates along the muscle fiber away from the neuromuscular junction. This electrical signal enters the transverse tubular network and in near synchrony activates the voltage sensors, the dihydropyridine receptors (DHPRs).* Activation of the DHPRs causes the opening of the ryanodine receptor $Ca^{2+}$ release channels (RyRs) located in the membrane of the SR. The subsequent $Ca^{2+}$ release into the myoplasm results in activation of the contractile apparatus (for reviews see Schneider 1994; Melzer et al., 1995). The RyR $Ca^{2+}$ release channel is a large homotetrameric molecule (Inui et al., 1987); its two main structural features include 4–12 putative transmembrane domains at the COOH-terminal region and a bulky cytoplasmic domain at the $NH_2$-terminal region, referred to as the junctional foot (Takeshima et al., 1989). It has been shown that in addition to the II-III loop of the DHPR, which may modulate transverse tubular voltage–dependent RyR activation (Tanabe et al., 1990, Nakai et al., 1998), $Ca^{2+}$ release from RyR in skeletal muscle is modulated by endogenous ligands such as $Ca^{2+}$ and $Mg^{2+}$ (Lamb and Stephenson, 1991; Meissner, 1994; Lacampagne et al., 1998) as well as regulatory proteins such as calmodulin and FKBP12 (Jayaraman et al., 1992; Timerman et al., 1993; Chen and MacLennan, 1994). Although, putative binding sites for these modulators have been determined, the question of how these stimuli are received and interpreted by the RyR remains largely unresolved.

The ability of cytosolic factors to affect $Ca^{2+}$ release suggests that the junctional domain of the RyR contains regulatory regions that receive, interpret, and transmit the modulatory signals. It is feasible that trans-

Address correspondence to Martin F. Schneider, University of Maryland School of Medicine, Department of Biochemistry and Molecular Biology, 108 North Greene Street, Room 229, Baltimore, MD 21201. Fax: (410) 706-8297; E-mail: mschneid@umaryland.edu

*Abbreviations used in this paper:* CICR, $Ca^{2+}$-induced $Ca^{2+}$-release; DHPR, dihydropyridine receptors; FDHM, full duration at half maximum amplitude; FWHM, full width at half maximum amplitude; MH, malignant hyperthermia.



Downloaded from http://rupress.org/jgp/article-pdf/119/1/15/1216418/8439.pdf by guest on 16 May 2022

mission of these signals is achieved through large conformational changes of the $Ca^{2+}$ release channel. Parallel investigations of conformational changes of the RyRs and $Ca^{2+}$ release have demonstrated that RyRs undergo large conformational changes before their opening and subsequent $Ca^{2+}$ release (El-Hayek et al., 1995). These conformational changes could be elicited even when $Ca^{2+}$ release is completely blocked by $Mg^{2+}$. Further evidence for large changes in conformation of the junctional as well as transmembrane regions of the skeletal RyRs was provided by electron cryomicroscopy and angular reconstitution techniques, which determined the 3-D structure of the skeletal muscle $Ca^{2+}$ release channel in closed, partially open, and fully open states (Serysheva et al., 1999; Sharma et al., 2000).

It is possible that domain–domain interactions within the RyRs may be involved in the intra-molecular signal transduction. Some of the regions proposed to be involved in these interdomain interactions, include those, which contain mutation sites for malignant hyperthermia (MH; for review see Mickelson and Louis, 1996). These mutation sites are generally restricted to the $Cys^{35}$-$Arg^{614}$ region of the RyR, designated as the $NH_2$-terminal domain, and the $Arg^{2168}$-$Arg^{2458}$ region, designated as central domain. Point mutations within specific positions of these domains produce functional modifications that are characterized by an enhanced activation by $Ca^{2+}$ (*i.e.*, $Ca^{2+}$-induced $Ca^{2+}$-release [CICR]; Ohta et al., 1989), and by increased sensitivity to RyR agonists (Mickelson et al., 1988, 1990). Recent investigations by El-Hayek et al. (1999) and Yamamoto et al. (2000) provided new evidence for involvement of these regions in interdomain interactions. In their report Yamamoto et al. (2000) demonstrated that synthetic peptides, which resemble either a segment of the $NH_2$-terminal domain ($Leu^{590}$-$Cys^{609}$), designated as domain peptide-1 (DP1), or a segment of the central domain of the junctional foot ($Leu^{2442}$-$Pro^{2477}$), designated as domain peptide-4 (DP4), enhance [$^3$H]ryanodine binding to the RyR $Ca^{2+}$ release channels, which is indicative of increased channel opening, and induce rapid $Ca^{2+}$ release. Presumably domain–domain interactions between the $NH_2$-terminal and central domains are engaged in stabilizing a closed state of the channel. It has been suggested that DP1 and DP4 bind to the $Ca^{2+}$ release channel by mimicking their respective RyR regions, thus preventing the interdomain interaction that occurs in the absence of added peptide. The resulting destabilization of the closed state may cause the channel to be more susceptible to activation by CICR, which may correspond to a functional state similar to that seen in channels with MH mutations. Interestingly, replacement of Arg of DP4 for Cys, (mimicking the in vivo mutation of $Arg^{2458}$-to-$Cys^{2458}$ in MH) abolished the effects of the peptide. These results provide new evidence that interdomain interactions may play an important role in the intramolecular signal transduction and regulation of $Ca^{2+}$ release from the SR. A recent report by Lamb et al., (2001) has also demonstrated that DP4 can substantially potentiate $Ca^{2+}$ release and force response to caffeine in mechanically peeled muscle fibers, without a significant effect on the properties of the contractile apparatus.

In the present study, we have investigated the effect of DP4 on localized $Ca^{2+}$ release events ($Ca^{2+}$ sparks) in permeabilized frog skeletal muscle fibers. We have also determined the effects of DP4 on [$^3$H]ryanodine binding to frog skeletal RyRs and examined single-channel properties in the presence of DP4 using frog RyRs reconstituted in planar lipid bilayers. We found that DP4 increased $Ca^{2+}$ spark frequency without appreciably altering the properties of the $Ca^{2+}$ sparks, increased [$^3$H]ryanodine binding to the frog SR vesicles and increased the open probability of frog RyR $Ca^{2+}$ release channels in bilayers. We have also determined that $Mg^{2+}$ modulates the effectiveness of DP4 in increasing the spark frequency, and that frog RyRs may have lower affinity for this peptide compared with their mammalian counterparts. Our findings are consistent with the hypothesis that the $Leu^{2442}$-$Pro^{2477}$ region of RyR1 is involved in an interdomain interaction that stabilizes the closed state of the RyR $Ca^{2+}$ release channel in skeletal muscle.

## MATERIALS AND METHODS

### *Peptide Synthesis*

Peptides were synthesized on a synthesizer (model 431A; Applied Biosystems) using Fmoc (*N*-(9-fluorenyl)methoxycarbonyl) as the α-amino protecting group. The peptides were cleaved and deprotected with 95% trifluoroacetic acid and purified by reversed-phase high pressure liquid chromatography. The amino acid sequence and the residue numbers corresponding to the in vivo sequence of the RyR1 are shown in Table I.

### *Fluorescence Measurements*

Experimental procedure and data analysis were performed as described by Shtifman et al. (2000). Briefly, cut segments of single fibers were isolated from *ileofibularis* muscle of frogs (*Rana pipiens*). Frogs were cooled in an ice bath and killed by decapitation and subsequent spinal cord destruction following protocols approved by the University of Maryland Institutional Animal Care and Use Committee. Removed muscle was pinned in a dissecting chamber containing Ringer's solution. Single fiber segments

TABLE I

*Amino Acid Sequence of the Synthetic Peptides Corresponding to the Selected Subdomains of Rabbit RyR1*

| Domain peptide | Corresponding domain of the RyR1 |
|---|---|
| DP4 | $^{2442}$LIQAGKGEALRIRAIL**R**SLVPLDDLVGIISLPLQIP$^{2477}$ |
| DP4mut | $^{2442}$LIQAGKGEALRIRAIL**C**SLVPLDDLVGIISLPLQIP$^{2477}$ |



Downloaded from http://rupress.org/jgp/article-pdf/119/1/15/1216418/8439.pdf by guest on 16 May 2022

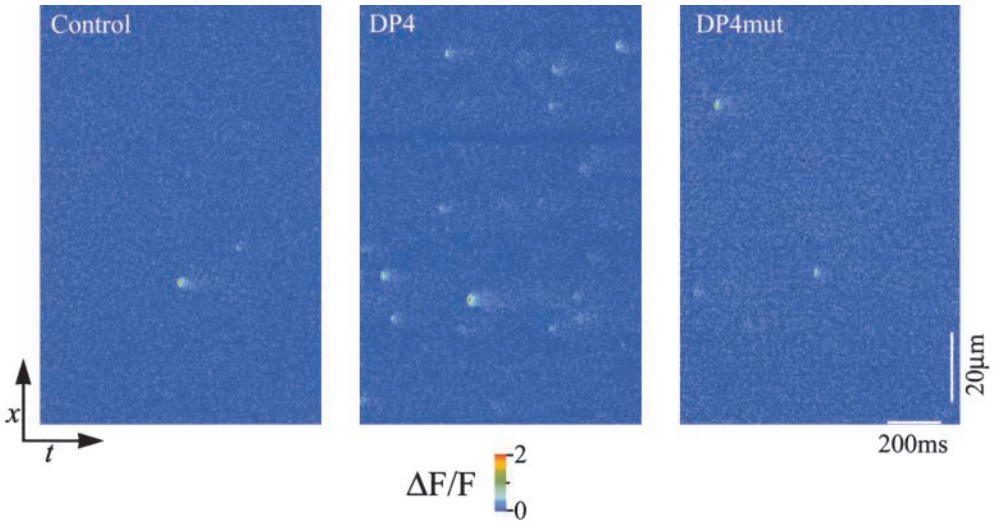


FIGURE 1. Effects of DP4 on $Ca^{2+}$ sparks in frog skeletal Muscle. Representative line-scan images under control, DP4 (50 μM) and DP4mut (50 μM) conditions. All fibers were bathed in internal solution ± peptide ($[Mg^{2+}]_{free}$1.2 mM) for 15 min before the start of image acquisition. The distance along the fiber ($x$) is represented vertically and the time ($t$) is represented horizontally to give the $x$ versus $t$ image in each panel.

(3–5 mm) were, manually dissected in the relaxing solution containing the following (in mM): 120 potassium glutamate, 2 $MgCl_2$, 0.1 EGTA, and 5 Na-Tris-maleate, pH 7.00. Cut fiber segments were mounted under stretch in a custom chamber as described by Lacampagne et al. (1998). The chemical permeabilization was realized by exposing the fiber to the relaxing solution containing 0.01% saponin for 35 s. The solution in the chamber was changed to an internal solution containing the following (in mM): 80 cesium glutamate, 20 creatine phosphate, 4.5 Na-Tris-maleate, 13.2 Cs-Tris-maleate, 5 glucose, 0.1 EGTA, 3 DTT, 0.05 Fluo-3 (pentapotassium salt) (Molecular Probes, Inc.), 4–10 $MgCl_2$ (0.25–3.01 $[Mg^{2+}]_{free}$), and 5 Na-ATP. Estimated $[Ca^{2+}]_{free}$ was 0.1 μM. To avoid the osmotic effects of chemical permeabilization, 8% dextran (41 K) was added to the solution (Tsuchiya, 1988; Ward et al., 1998). Line-scan images were computer processed to automatically identify and store spark locations using a relative threshold algorithm as described by Cheng et al. (1999) and further analyzed as previously described by our laboratory (Lacampagne et al., 1998; Shtifman et al., 2000).

### *Preparation of Skeletal Microsomes*

For the preparation of frog muscle homogenates, leg muscle was homogenized in a Waring blender at high speed with four volumes (per muscle weight) of 20 mM MOPS, pH 7.2, 0.1 mM PMSF, and 2 μg/ml trypsin inhibitor for 5 × 20 s with a 5-min interval. After each step of homogenization, the pH was adjusted to 7.0 using NaOH. After homogenization, coarse debris was removed using a needle.

### *[$^3$H]Ryanodine Binding Assay*

The muscle homogenates (1.0 mg/ml) were incubated in 0.1 ml of a reaction solution containing 10 nM [$^3$H]ryanodine (68.4 Ci/ml; DuPont), 0.15 M KCl, 10 μM of $CaCl_2$, and 20 mM MOPS, pH 7.2, for 2 h at 37°C in the presence of various concentrations of peptides. Samples were filtered onto glass fiber filters (GF/A; Whatman) and washed three times with 5 ml of distilled water. Filters were placed in scintillation vials containing 10 ml of scintillation cocktail Ecoscint A and counted in a Beckman counter (model LS 3801). Specific binding was calculated as the difference between the binding in the absence (total binding) and in the presence (nonspecific binding) of 10 μM nonradioactive ryanodine. Assays were performed in duplicate.

### *Single-channel Recordings in Planar Lipid Bilayers*

Reconstitution of frog skeletal muscle SR vesicles into planar lipid bilayers for single-channel recordings of RyRs was performed as described before (Shtifman et al., 2000). Briefly, a bilayer of phosphatidylethanolamine/phosphatidylserine (1:1 dissolved in $n$-decane to 25 mg/ml) was "painted" with a glass rod across an aperture of ~250 μm diameter in a delrin cup. The cis chamber was the voltage control side connected to the head stage of a 200-A amplifier (Axopatch), whereas the trans side was held at virtual ground. The cis (500 μl) and trans (600 μl) chambers were initially filled with 50 mM cesium methanesulfonate and 10 mM Na-HEPES, pH 7.2. After bilayer formation, an asymmetric cesium methanesulfonate gradient (300 mM cis/50 mM trans) was established and the SR vesicles were added to the cis chamber, which corresponded to the cytoplasmic side of the SR, whereas the trans side corresponded to the lumenal side. Contaminant $Ca^{2+}$ (3–5 μM) was sufficient to elicit channel activity. After detection of channel openings, $Cs^+$ in the trans chamber was raised to 300 mM to dissipate the chemical gradient and prevent further vesicle fusion. For each condition, single-channel data were collected at steady voltages (+30 and −30 mV) for 2–4 min. Signals were analyzed after filtering with an 8-pole low pass Bessel filter at a sampling frequency of 1.5–2 kHz. Data acquisition and analysis were done with Axon Instruments software and hardware (pClamp v6.0.3; Digidata 1200 AD/DA interface).

### *Data Analysis*

All Results are expressed as mean ± SEM. Linear regression (least-squares fit) and all nonlinear curve fitting routines were performed using ORIGIN 6.0. (Microcal) Statistical analysis for the comparison of values was performed using an analysis of variance test (ANOVA). $P < 0.05$ was accepted as statistically significant.

## RESULTS

### *DP4 Increases $Ca^{2+}$ Spark Frequency*

To investigate the effects of DP4 and DP4mut on localized $Ca^{2+}$ release, permeabilized, cut skeletal muscle fibers were incubated in parallel in either an internal solution (control) or in an internal solution containing the appropriate concentration of either peptide.



Downloaded from http://rupress.org/jgp/article-pdf/119/1/15/1216418/8439.pdf by guest on 16 May 2022

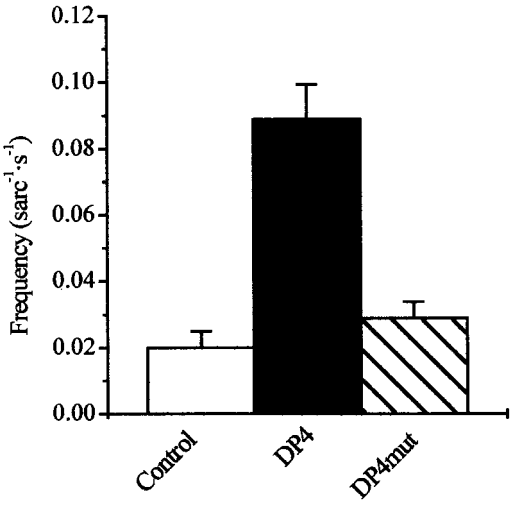


FIGURE 2. DP4 increases $Ca^{2+}$ spark frequency in frog skeletal muscle fibers. $Ca^{2+}$ spark frequency detected in the fibers described in Fig. 1. Bars represent the mean ± SEM of six experiments performed in each condition.

Fig. 1 shows representative line-scan fluorescence (ΔF/F) images of permeabilized frog muscle fibers in control and after addition of either 50 μM DP4 or 50 μM DP4mut to the bathing solution. Each image was obtained from a set of five 1-s duration line-scan images recorded with ~1 s separation between successive images. The distance along the fiber ($x$) is represented vertically and the time ($t$) is represented horizontally to give the $x$ versus $t$ image in each panel. Multiple successive runs of images were recorded in each condition. To avoid laser damage, the scan line was moved 1.8 μm perpendicular to the long axis of the fiber after each run. Each localized increase in $[Ca^{2+}]$ ($Ca^{2+}$ spark) is characterized by a brief and localized increase in fluorescence (Klein et al., 1996; Schneider and Klein, 1996). When added to the permeabilized muscle fibers, DP4 appeared to modulate SR $Ca^{2+}$ release by producing a large increase in the frequency of $Ca^{2+}$ sparks (Figs. 1 and 2). Contrary to the effects of DP4, addition of DP4mut did not produce an appreciable increase in $Ca^{2+}$ spark frequency (Figs. 1 and 2), suggesting that $Arg^{2458}$ of RyR ($Arg^{17}$ of DP4) plays a critical role in stabilizing interdomain interaction within the channel.

We next analyzed parameters of individual $Ca^{2+}$ release events to determine if the increase in the event frequency produced by DP4 was also accompanied by any changes in the properties of these events. Analysis of the spark properties in all tested conditions in Fig. 3 demonstrated that $Ca^{2+}$ spark properties were slightly but statistically significantly different in the absence and in the presence of the peptides. However, in all tested conditions, these differences in 50 μM DP4 were never >5%, whereas the change in spark frequency in the same experiments was >300%. As demonstrated in Fig. 4, the amplitude distribution of $Ca^{2+}$ release events as well as the distributions of rise times, FWHM, and FDHM were also highly similar in control and DP4 conditions. As presented in Figs. 1 and 2, binding of DP4 causes the channel to become more susceptible to activation, thereby mimicking the MH condition. According to previous reports, human and porcine RyR $Ca^{2+}$ release channels carrying MH mutations do not exhibit altered channel conductance or gating properties (Fill et al., 1991; Shomer et al., 1993, 1994). As presented here, the major parameters underlying a typical $Ca^{2+}$ spark, which directly relate to the gating and conductance properties of an open $Ca^{2+}$ release unit, namely the rise time and the peak amplitude, were closely similar in control fibers and in fibers bathed with DP4.

### *Concentration Dependence of DP4 Effects in Muscle Fibers*

Fig. 5 A demonstrates that DP4 elicited an increase in $Ca^{2+}$ spark frequency in permeabilized muscle fibers in

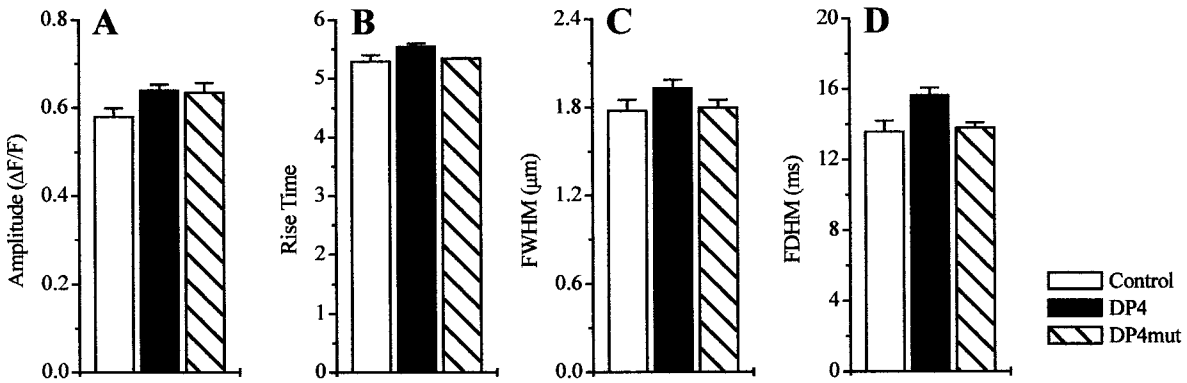


FIGURE 3. Effect of DP4 on individual event properties $Ca^{2+}$ spark event properties under control ($n_{events}$ = 1317), DP4 ($n_{events}$ = 2,590), and DP4mut ($n_{events}$ = 717) in the fibers described in Figs. 1 and 2. Each panel represents $Ca^{2+}$ release event ΔF/F amplitude (A), 10–90% rise time (B), full width at half maximum amplitude (FWHM) (C), and full duration at half maximum amplitude (FDHM) (D). All properties are presented as mean ± SEM.



Downloaded from http://rupress.org/jgp/article-pdf/119/1/15/1216418/8439.pdf by guest on 16 May 2022

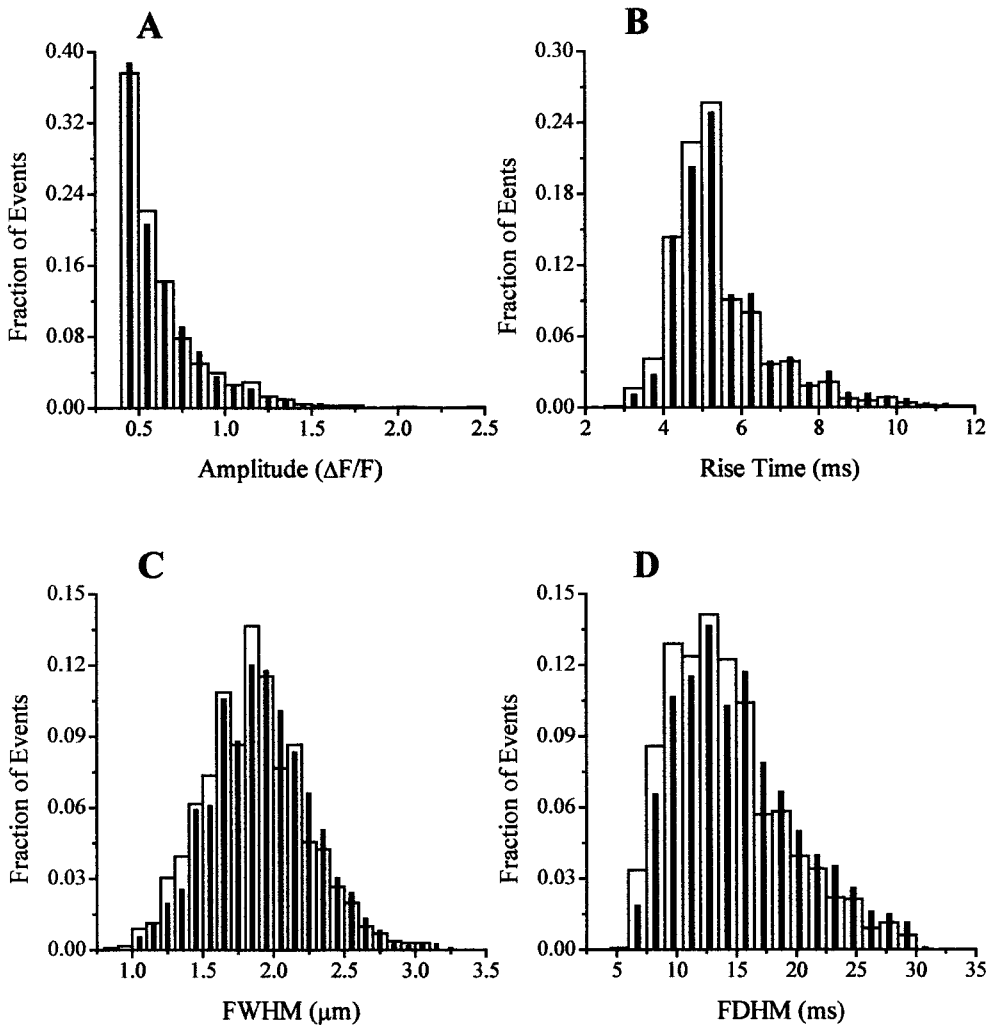


FIGURE 4. Effect of DP4 on distribution of $Ca^{2+}$ spark parameters. Normalized histograms of amplitudes (A), rise times (B), FWHM (C), and FDHM (D) obtained under control (open bars) or DP4 (50 μM; filled bars) condition. Same number of events as noted in Fig. 3.

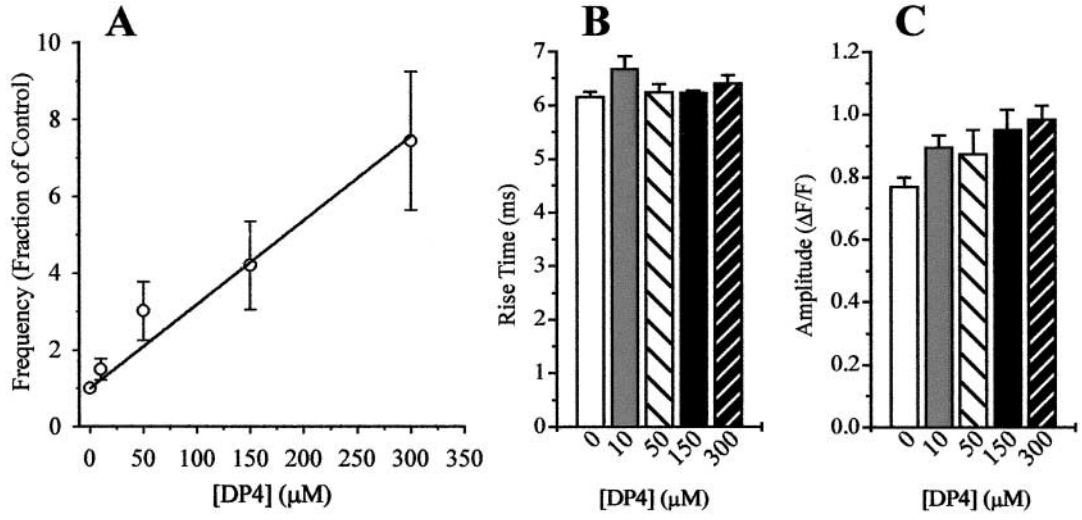


FIGURE 5. Dose response of DP4 effect in muscle fibers. (A) Frequency of $Ca^{2+}$ sparks detected under control and various concentrations of added DP4. All recordings were initially made while the fibers were bathed in an internal solution ($[Mg^{2+}]_{free}$ = 1.2 mM) in which the mean spark rate was 0.018 ± 0.006 $sarc^{-1}$ $s^{-1}$. The solution was later exchanged to the same internal solution with added DP4 (10, 50, 150, or 300 μM). All fibers were bathed in DP4-containing solution for 15 min before the image acquisition. $Ca^{2+}$ spark frequency at each [DP4] was normalized to the frequency in the control condition from the same fiber. $Ca^{2+}$ spark amplitude (B) and rise time properties (C) obtained from the fibers described in Fig. 5 A. All data points are presented as mean ± SEM.



Downloaded from http://rupress.org/jgp/article-pdf/119/1/15/1216418/8439.pdf by guest on 16 May 2022

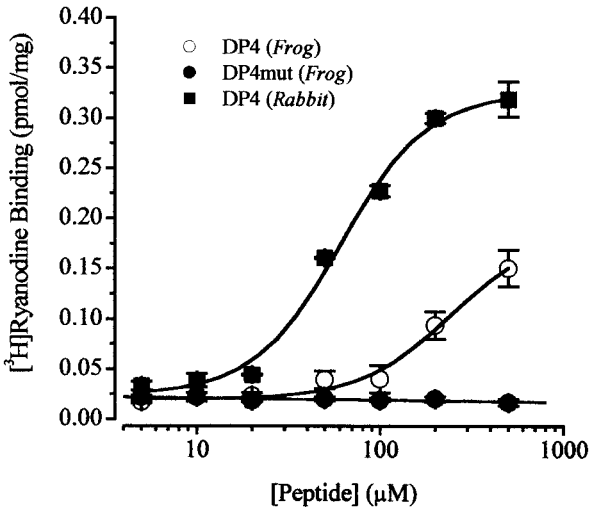


FIGURE 6. DP4 enhances [$^3$H]ryanodine binding to rabbit and frog skeletal muscle microsomes. Rabbit skeletal and frog skeletal muscle microsomes were incubated at various concentrations of DP4, as indicated (MATERIALS AND METHODS). Ryanodine binding in the absence of peptides was 0.03 pmol/mg for the rabbit and 0.015 pmol/mg for frog microsomes. DP4mut did not enhance [$^3$H]ryanodine binding in all tested concentrations. Each datum point represents the mean ± SEM of three experiments performed in duplicate. DP4 data was best fit to a sigmoidal function, whereas the DP4 mutant was best fit by a linear least-squares regression.

a dose-dependent manner. In these experiments, which followed a different protocol than the experiments described in Figs. 1–4, the initial set of control images was acquired while the fibers were bathed in a DP4-free internal solution with 1.2 mM $[Mg^{2+}]_{free}$ (MATERIALS AND METHODS). This solution was exchanged for the same internal solution containing either 0, 10, 50, 150, or 300 μM added DP4. Fibers were incubated in DP4-containing solution for 15 min before the start of image acquisition. Images in each condition were acquired at different positions along the fiber to avoid possible laser damage. Each data point in Fig. 5 A was normalized to the $Ca^{2+}$ spark frequency in the same fiber in the control condition (i.e., [DP4] = 0 μM) to account for the variability in resting frequency between different fibers and for potential differences in SR $Ca^{2+}$ load. As seen in this figure, increasing [DP4] up to 300 μM caused a linear increase in spark frequency, which never achieved a saturating level. Thus, the apparent affinity of DP4 for the RyR was relatively low in the muscle fiber experiments, with apparent dissociation constant considerably >300 μM (Fig. 5 A). Statistical analysis of $Ca^{2+}$ spark amplitude and rise time at each [DP4] has demonstrated that these spark properties did not change with the increasing concentration of the peptide (Fig. 5, B and C).

*Effects of DP4 on [$^3$H]Ryanodine Binding to Mammalian and Frog RyRs*

Fig. 6 presents the data of [$^3$H]ryanodine binding to the SR vesicles isolated from frog and mammalian skeletal muscle in the presence of different concentrations of DP4 and DP4mut. Addition of DP4 produced a pronounced enhancement of [$^3$H]ryanodine binding to both mammalian (RyR1) and frog (RyRα and RyRβ) preparations in a concentration-dependent manner. DP4mut produced no appreciable effect on ryanodine binding to frog (Fig. 6) or mammalian preparations previously described by Yamamoto et al. (2000) at all tested concentrations. Unlike the mammalian preparation, where a maximal effect was achieved at [DP4] of ~500 μM ($AC_{50}$ = 53 μM), the enhancement of ryanodine binding in the frog preparation was much smaller over the same range of tested concentrations of DP4. The nonsaturable dependence of DP4 could be a consequence of a narrower gap between the interacting domains in the frog RyR compared with the rabbit RyR.

*Modulation of DP4 Effects by $Mg^{2+}$ in Muscle Fibers*

To test whether $Mg^{2+}$ has a modulatory effect on DP4 activity, we conducted a series of assays, similar to those described in Fig. 5, using 0.25, 0.65, 1.2, and 1.87 mM $[Mg^{2+}]_{free}$ over the range of DP4 concentration (0–300 μM). To compare results from different fibers, each fiber was first studied under a control condition (1.2 mM

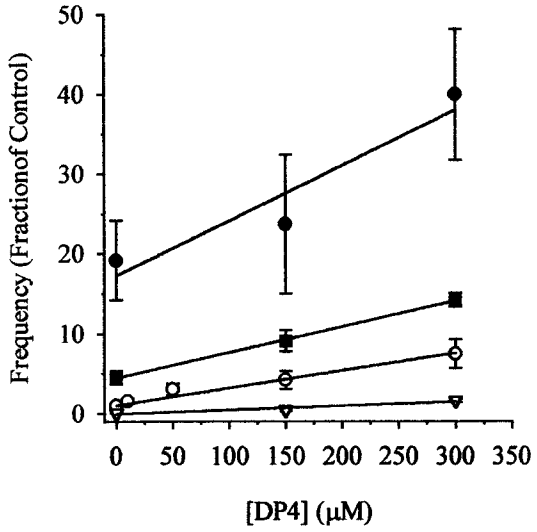


FIGURE 7. Effect of $[Mg^{2+}]$ on $Ca^{2+}$ spark frequency in presence of DP4. Experiments were performed as described in Fig. 6 at $[Mg^{2+}]_{free}$ 0.25 mM (closed circle), 0.65 mM (filled square), 1.2 mM (open circles), and 1.87 mM (open triangle). Each datum point represents three or more experiments performed in each condition. Each condition was fit with a linear regression function by the least-squares method. Statistical analysis for the comparison of slopes was performed using an analysis of covariance test (ANOVA). $P < 0.05$ was accepted as statistically significant.



Downloaded from http://rupress.org/jgp/article-pdf/119/1/15/1216418/8439.pdf by guest on 16 May 2022

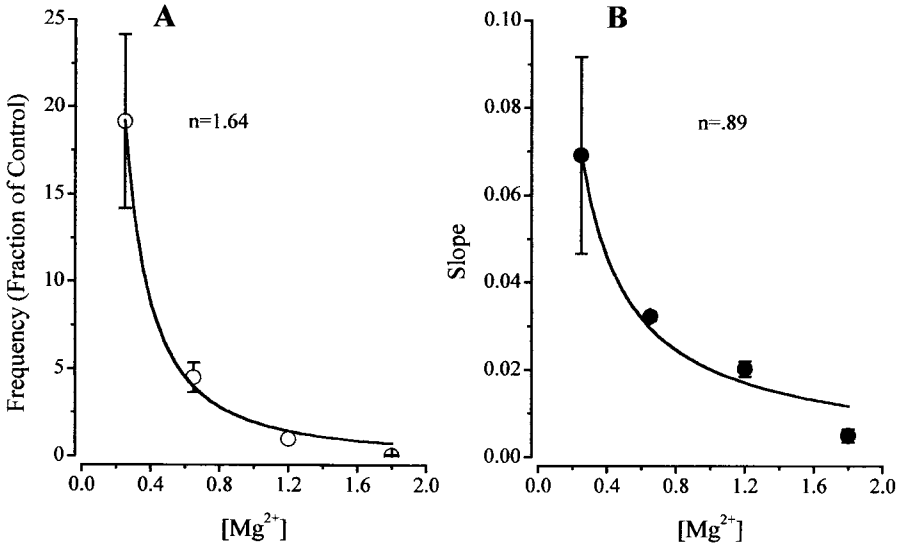


FIGURE 8. $Mg^{2+}$ dependence of spark frequency and effectiveness of DP4 in muscle fibers. (A) $[Mg^{2+}]$ dependence of SR $Ca^{2+}$ release event frequency under control condition obtained from Fig. 7. (B) The $[Mg^{2+}]$ dependence of the slope of the DP4 induced $Ca^{2+}$ spark frequency response. Slope (B) represents change in normalized frequency per micromolar DP4 (Fig. 7), and has units of fraction of control/ μM. Data have been fitted by $f = K/[Mg^{2+}]^n$, with K = 1.9, n = 1.64 in A and K = 0.02, n = 0.89 in B.

$[Mg^{2+}]_{free}$ and [DP4] = 0 μM), and then under another condition with the appropriate $Mg^{2+}$ and DP4 concentration (Fig. 7). The spark frequency at each condition was normalized to the frequency under the control condition in the same fiber. As demonstrated here, we observed an increase in the $Ca^{2+}$ spark frequency that increased linearly in response to increasing [DP4] at all tested $Mg^{2+}$ conditions. Statistical analysis of fits through the points in each $[Mg^{2+}]$ condition has demonstrated that increasing concentrations of cytosolic $[Mg^{2+}]_{free}$ steadily decreased the slope of the dose response to DP4.

Fig. 8 A summarizes the effect of $[Mg^{2+}]$ on $Ca^{2+}$ spark frequency in the absence of DP4. As described above, all experiments were performed initially with our standard solution ($[Mg^{2+}]_{free}$ = 1.2 mM) that was later exchanged for a solution containing a different concentration of $Mg^{2+}$. The spontaneous event frequency was almost completely inhibited by 1.87 mM $Mg^{2+}$. However, decreasing the concentration of cytosolic $Mg^{2+}$ resulted in a steep increase in $Ca^{2+}$ spark frequency. As described by Lacampagne et al. (1998), the binding of $Mg^{2+}$ to SR $Ca^{2+}$ release channels and the consequent inhibition of the rate of $Ca^{2+}$ release events, can be described by the Eq. 1:

$$f = K/[Mg^{2+}]^n, \quad (1)$$

where $f$ is the observed event frequency, $n$ is a lower bound for the number of interaction sites, and K is a constant equal to $f_{max} \cdot K_d^n$. This equation is based on the assumption that $K_d \ll [Mg^{2+}]$, which may be realized for the high affinity (A) sites by the fact that $[Mg^{2+}]$ used in all of our experiments is well above the predicted $K_d$ for $Mg^{2+}$ at the high affinity binding site on the RyR (75 μM; Ogawa et al., 2000). However, this relationship may not be strictly realized for the low affinity (I) $Mg^{2+}$ binding sites that have a predicted $K_d$ of 0.3 mM for $Mg^{2+}$ (Ogawa et al., 2000; see model simulation below). Normalizing to the frequency in the standard solution gives

$$f/f_{std} = ([Mg^{2+}]_{std}/[Mg^{2+}])^n, \quad (2)$$

where $f_{std}$ and $[Mg^{2+}]_{std}$ are the frequency and $[Mg^{2+}]$(=1.2 mM) in the standard solution.

Using Eq. 2, the results in Fig. 8 A have been fitted as indicated by the line on the graph. The results of the fit gave a value for $n$ = 1.64, which is consistent with previous results (Lacampagne et al., 1998), suggesting that two $Mg^{2+}$ binding sites on the RyR have to be free of $Mg^{2+}$ to remove the inhibitory effect of $Mg^{2+}$ on $Ca^{2+}$ spark frequency.

The data in Fig. 8 B summarize the effect of $[Mg^{2+}]$ on the [DP4] dependence of $Ca^{2+}$ spark frequency. An equation similar to Eq. 1, but with f replaced by the slope of the response to DP4, can be applied to characterize the $Mg^{2+}$ dependence of the effectiveness of this peptide to activate $Ca^{2+}$ sparks. The results of the fit of this equation to the data (Fig. 8 B) gave a value for $n$ = 0.89, suggesting that only a single $Mg^{2+}$ binding site is involved in modulation of DP4 effectiveness.

### *A Reaction Scheme for Modulation of DP4 Effects by $Mg^{2+}$*

Since all of the present $Ca^{2+}$ spark experiments were conducted with permeabilized, and thus depolarized muscle fibers, it seems appropriate to assume that all of the detected events were produced by the CICR mechanism and not by voltage sensor activation (Schneider and Klein, 1996). CICR in skeletal muscle cells is regu-



Downloaded from http://rupress.org/jgp/article-pdf/119/1/15/1216418/8439.pdf by guest on 16 May 2022

lated biphasically by $Ca^{2+}$. Micromolar [$Ca^{2+}$] activates the RyR $Ca^{2+}$ release channels, whereas millimolar [$Ca^{2+}$] inactivates the RyRs. This type of regulation suggests that there are two distinct types of $Ca^{2+}$ binding sites on the RyR: (1) the high affinity, activating site (A-site) and (2) the low affinity, inactivating site (I-site). In practice, $Ca^{2+}$ binding to the I-site would be negligible at the physiological [$Ca^{2+}$] levels (submicromolar) characteristic of resting muscle and used in the present permeabilized fiber studies. However, the extent of CICR also depends on $Mg^{2+}$. At physiological concentrations (~1 mM) $Mg^{2+}$ can inhibit $Ca^{2+}$ release by acting as a competitive antagonist of $Ca^{2+}$ binding at the A-site and/or as a competitive agonist with $Ca^{2+}$ for interaction at the I-site (Laver et al., 1997a). It has been suggested that decreasing the occupancy of the A-site by $Mg^{2+}$, and consequent increase in the occupancy of the same site by $Ca^{2+}$ is responsible for CICR activation of $Ca^{2+}$ sparks when cytosolic [$Mg^{2+}$] is reduced in muscle (Lacampagne et al., 1998).

The top line of Scheme I represents divalent cation regulation of the RyR $Ca^{2+}$ release channel in the absence of DP4. Dissociation of $Mg^{2+}$ (green) from the I and A-sites is followed by activation of the RyR $Ca^{2+}$ release channel by $Ca^{2+}$ (red) binding to the A-site of the divalent cation-free RyR. For simplicity, Scheme I uses sequential dissociation of Mg from the I- and then the A-sites rather than parallel independent binding, since in practice when investigating the effects of lowering [$Mg^{2+}$], the lower affinity I-site would lose $Mg^{2+}$ at higher [$Mg^{2+}$] than the higher affinity A-site. Under resting conditions, the ambient cytosolic [$Ca^{2+}$] is too low for appreciable binding of $Ca^{2+}$ to the I-site.

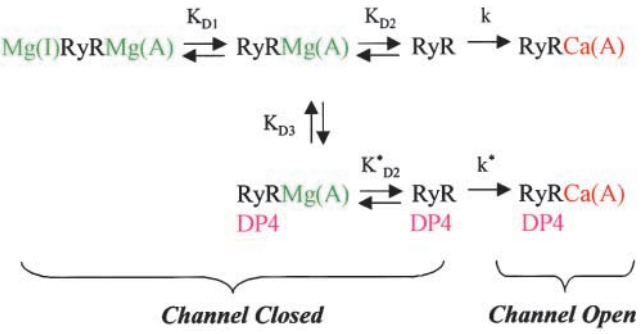


(SCHEME I)

Using values for the dissociation constants for $Mg^{2+}$ from the I and A-sites (Scheme I, $K_{D1}$ and $K_{D2}$, respectively) that were half of the values given for the equivalent dissociation constants used by Ogawa et al. (2000) for skinned muscle fibers in a parallel (i.e., independent) binding scheme, we can reproduce (Fig. 9 A) the [$Mg^{2+}$] inverse power dependence ($n$ = 1.70 in simulated results) of spark frequency observed experimentally in the absence of DP4 (Fig. 8 A; $n$ = 1.64). In these simulations, we assume that all available closed states are in equilibrium, and that the rate of occurrence of $Ca^{2+}$ sparks (equation in Fig. 9 legend) is proportional to the fraction of closed channels in the divalent cation-free state (RyR in the top line of Scheme I). The

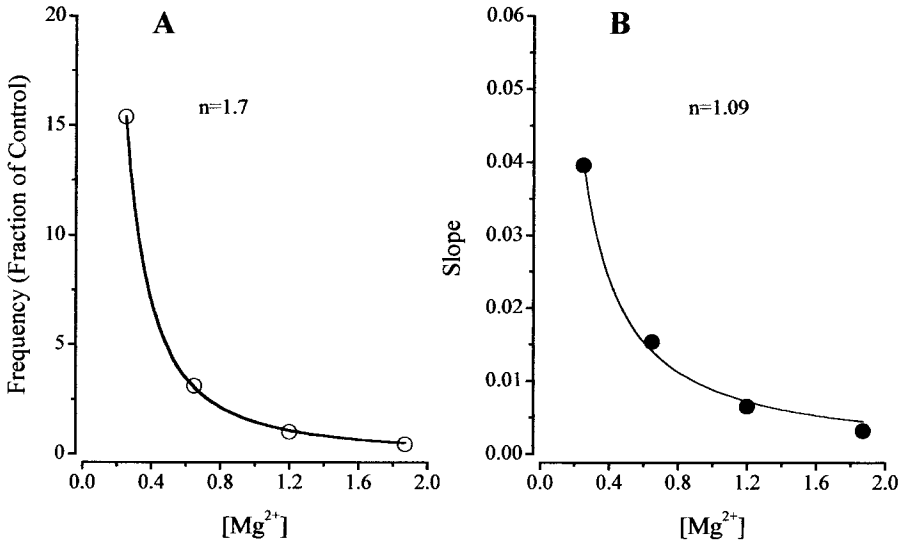


FIGURE 9. Simulation of $Mg^{2+}$ dependence of spark frequency and effectiveness of DP4 in muscle fibers. Simulated data based on the kinetic model described in Scheme I. For Scheme I, the relative rate of occurrence of $Ca^{2+}$ sparks is given by $(k \cdot K_{D2} \cdot K_{D3} + k^* \cdot K_{D2} \cdot [DP4])/(K_{D2} \cdot K_{D3} \cdot F + [Mg^{2+}] \cdot [DP4] + K_{D2}^* \cdot [DP4])$, where $F = ([Mg^{2+}]^2 + K_{D1} + [Mg^{2+}] + K_{D1} \cdot K_{D2})/K_{D1} \cdot K_{D2}$. The parameter values used for the simulation were $K_{D1}$ = 150 μM, $K_{D2} = K_{D2}^*$ = 37.5 μM, $K_{D3}$ = 100 μM and $k = k^*$. (A) Simulated [$Mg^{2+}$] dependence of SR $Ca^{2+}$ release event frequency under control conditions with no DP4 present normalized to the simulated frequency at 1.2 mM $Mg^{2+}$. (B) Simulated [$Mg^{2+}$] dependence of the slope of the DP4 induced $Ca^{2+}$ spark frequency response. As in Fig. 8, the slope (B) represents change in normalized frequency per micromolar DP4 (Fig. 7), and has units of fraction of control/μM. Data were fitted as described in Fig. 8.



Downloaded from http://rupress.org/jgp/article-pdf/119/1/15/1216418/8439.pdf by guest on 16 May 2022

equilibrium assumption seems reasonable since, in the $Ca^{2+}$ spark experiments, the rate of occurrence of sparks is so low that the occurrence of an opening event must be extremely rare. After opening, the channel presumably inactivates by $Ca^{2+}$-dependent inactivation (not shown), and then recovers from inactivation (not shown) to return to the total pool of available channels. The fraction of channels recovering from inactivation was assumed to be negligible.

We next consider the situation in the presence of DP4. The full reaction scheme (Scheme I), in which DP4 can only bind to the RyR after dissociation of $Mg^{2+}$ from the low affinity (I) site, also reproduces the results in Fig. 8 B. Note that in simulating the effects of DP4, we have not altered the parameter values in the top line of Scheme I, so the $Mg^{2+}$ effects in the absence of DP4 will continue to be reproduced (Fig. 9 A). For the simulation of DP4 effects, we assumed for simplicity that DP4 binding has no direct effect on the dissociation of $Mg^{2+}$ from the A-site or on the binding of $Ca^{2+}$ to the $Mg^{2+}$-free channel (i.e., $K_{D2} = K_{D2}^*$ and $k = k^*$). However, even under these assumptions, the presence of increasing [DP4] still promotes channel opening by preferential binding to the partially $Mg^{2+}$-free channel, and thus increasing the fraction of channels in the RyR or RyR-DP4 states. Fig. 9 B indicates that, under these assumptions, the model in Scheme I well reproduces the experimentally observed $[Mg^{2+}]$ dependence of the effectiveness of DP4 on $Ca^{2+}$ spark frequency (Fig. 8 B). Unlike Scheme I, an alternative reaction scheme in which DP4 binds only after dissociation of $Mg^{2+}$ from both the I and A-sites (not shown), gives a simulated $[Mg^{2+}]$ power dependence for the effectiveness of DP4 of ~1.7 (simulation not shown). This is about the same as the simulated $[Mg^{2+}]$ power dependence of spark frequency in the absence of DP4 (Fig. 9 A), which is contrary to the experimental observations (Fig. 8 B). Equal affinity binding of DP4 to all states in the top line of Scheme I would not alter spark frequency if $k = k^*$. Finally, adding the possibility of binding of DP4 to the divalent cation-free state RyR in Scheme I would not alter the fractional occupancy of states RyR or RyR-DP4 under equilibrium conditions (above), and would consequently be the same as Scheme I. Thus, preferential binding of DP4 after dissociation of $Mg^{2+}$ from the I-site appears to be the simplest possibility consistent with our experimental results.

The muscle fiber experiments were performed under conditions of low frequency of occurrence of $Ca^{2+}$ sparks. Scheme I successfully duplicates the effects of $Mg^{2+}$ and DP4 on spark frequency in these experiments under conditions of low spark frequency. Scheme I can thus successfully account for the equilibrium fraction of total $Ca^{2+}$ release channels occupying the divalent cation-free channel states (Scheme I, RyR and Dp4RyR) immediately preceding the channel-opening step that initiates a spark. With the parameter values used in Fig. 9, the simulated occupancy of channels in the divalent cation-free state (Scheme I, RyR) was only 0.3% under the reference conditions ($[Mg^{2+}] = 1.2$ mM and no DP4), and the maximum simulated total occupancy of the two divalent cation-free states (RyR and Dp4RyR, Scheme I) was only 2.4% (at $[Mg^{2+}] = 0.25$ mM and [DP4] = 300 μM), which is consistent with the low likelihood of occurrence of $Ca^{2+}$ sparks in our experiments.

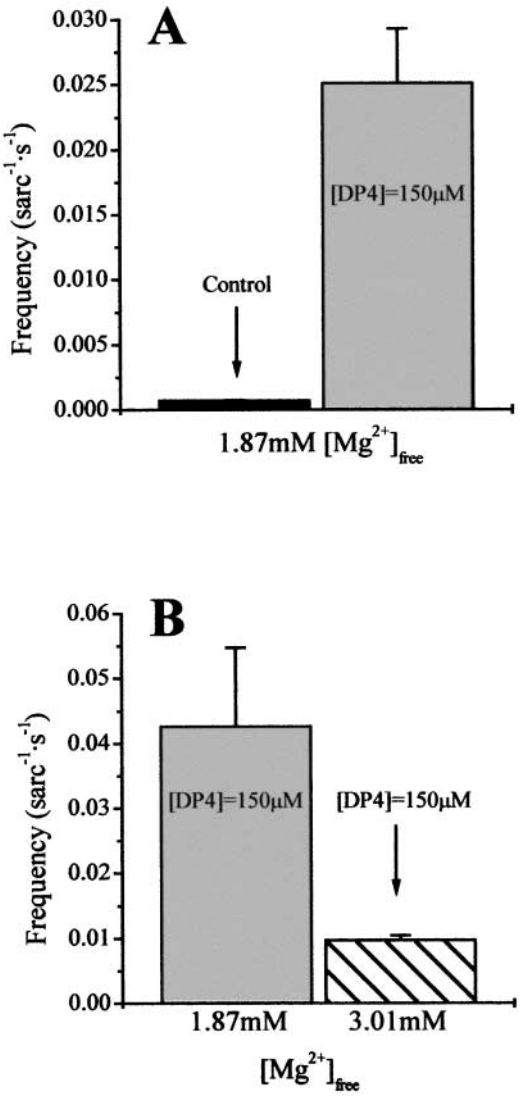


FIGURE 10. DP4 can overcome $Mg^{2+}$ inhibition. (A) The effect of addition of 150 μM DP4 (right) on $Ca^{2+}$ spark frequency in 1.87 mM $Mg^{2+}$. (B) Effect of increasing $Mg^{2+}$ from 1.87 mM (left) to 3.0 mM (right) on $Ca^{2+}$ spark frequency in the presence of 150 μM DP4. This figure demonstrates that in presence of high $[Mg^{2+}]$ (≥1.2mM), where resting $Ca^{2+}$ spark frequency was almost completely inhibited, DP4 was still able to elicit $Ca^{2+}$ release from the SR.



Downloaded from http://rupress.org/jgp/article-pdf/119/1/15/1216418/8439.pdf by guest on 16 May 2022

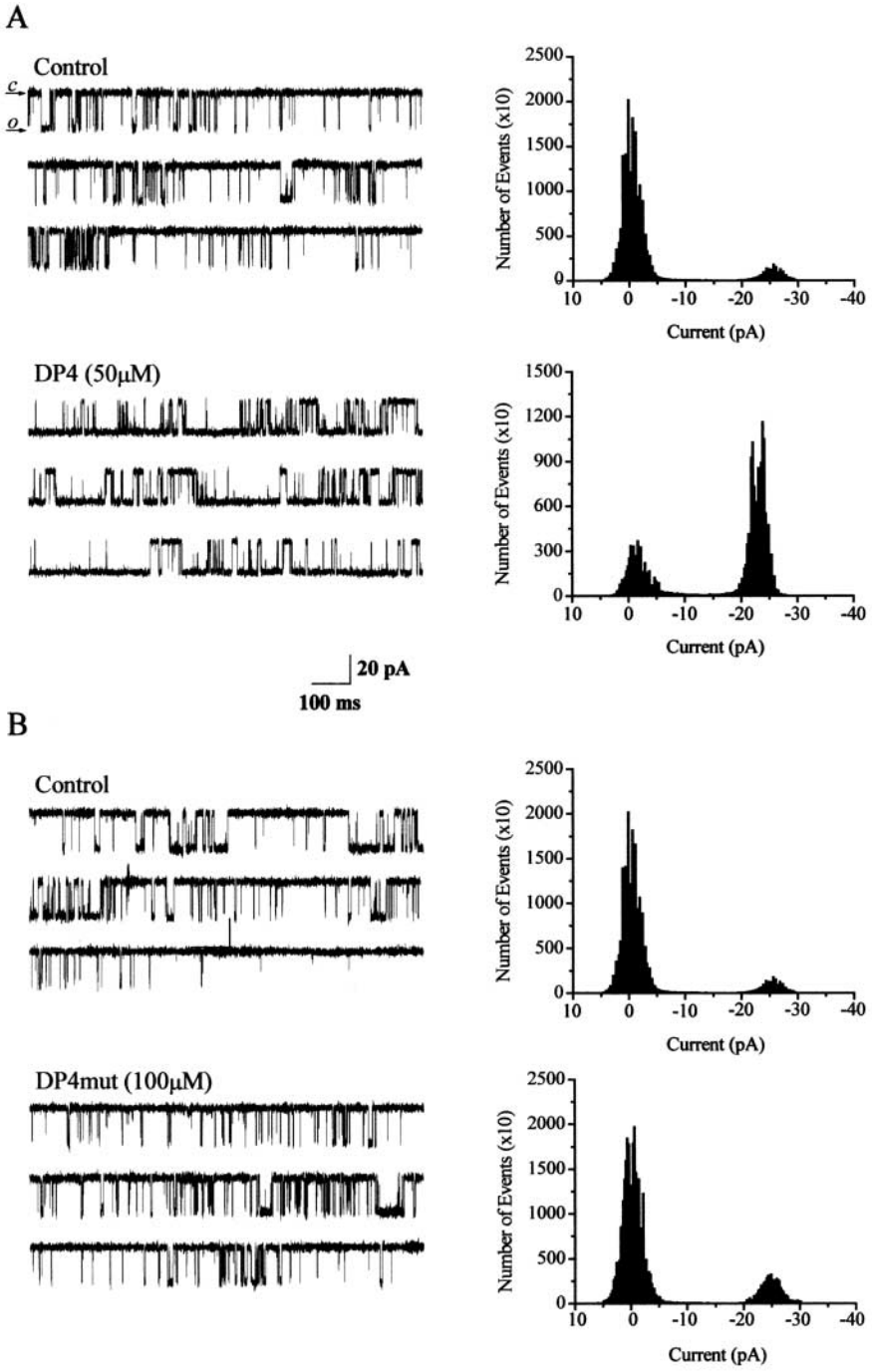


FIGURE 11. Effects of DP4 on single channels isolated from frog SR. (A) Single-channel traces (2 s each) of frog skeletal muscle RyR activity were obtained in the absence (control) and in the presence of 50 μM DP4 added to the cis (cytosolic) face of the channel. Downward deflections of the baseline current represent channel openings. (B) Another RyR channel recorded in the absence (control) and the presence of 100 μM. DP4 mutant added to the cis side of the channel. DP4 mutant did not exert any significant change in channel activity for the whole duration of the experiment (30 min). (Right panels) Current amplitude histograms for representative 60-s activity periods of the channel under the condition described above the traces. Holding voltage = +30mV. Symmetric solutions contained 300 mM cesium methanesulfonate and 10 mM Na-HEPES, pH 7.2, with no added $Mg^{2+}$ and pCa ~ 5. Scale bars: 30 pA (y-axis) and 300 ms (x-axis).

*DP4 Can Overcome Inhibition by $Mg^{2+}$*

To determine if DP4 can overcome $Mg^{2+}$ inhibition, we conducted a series of experiments under physiologically inhibitory conditions. It has been shown that $[Mg^{2+}]_{free}$ of 1.8 mM and higher almost completely inhibits $Ca^{2+}$ spark frequency in cut frog skeletal muscle fibers (Fig. 10 A) (Lacampagne et al., 1998). At this $[Mg^{2+}]$, the majority of the high affinity binding sites on the RyRs should be occupied. When applying 150 μM DP4 to fibers bathed in an internal solution containing either 1.87 (Fig. 10, A and B) or 3.01 mM $[Mg^{2+}]_{free}$ (Fig. 10 B), we consistently observed an appreciable increase in $Ca^{2+}$ spark frequency, whereas the frequency in the control condition was almost negligible (Fig. 10 A), suggesting that under these conditions all detected $Ca^{2+}$ sparks were produced solely due to interaction of DP4 with the channel. These results strongly indicate that the presence of DP4 at the channel can partially overcome inhibition of $Ca^{2+}$ release by $Mg^{2+}$. The relative increase in spark frequency observed on adding 150 μM DP4 to muscle fibers in 1.87



Downloaded from http://rupress.org/jgp/article-pdf/119/1/15/1216418/8439.pdf by guest on 16 May 2022

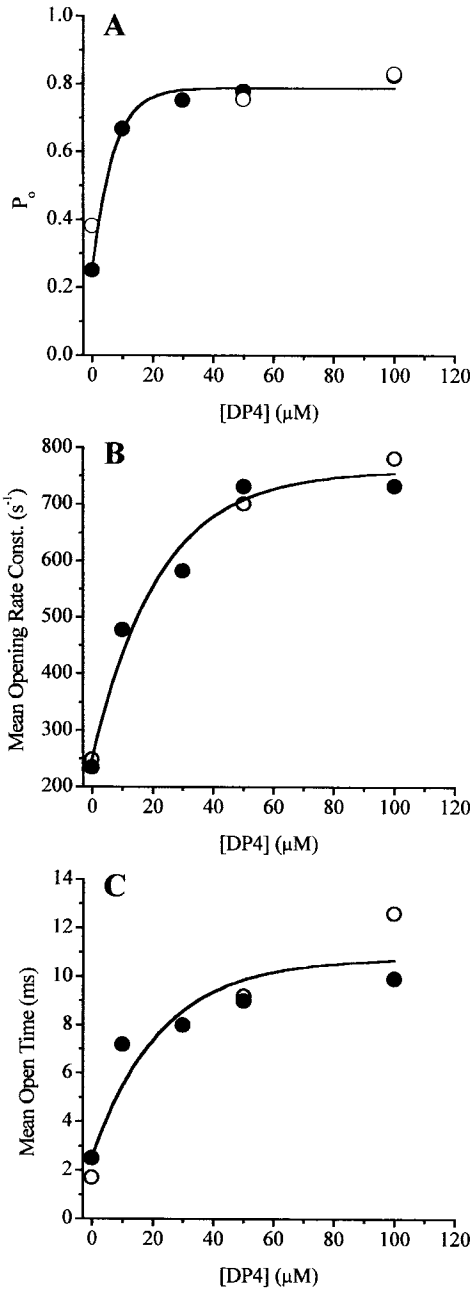


FIGURE 12. Dose response of DP4 effect on frog skeletal RyRs in bilayers. (A) Channel open probability as a function of [DP4] determined from single–channel recordings described in Fig. 11. Calculated mean opening rate (B) and mean open time (C) of the channels over the range of all tested [DP4]s, using formula $[(1/\tau_{1\ closed}) \cdot f_1] + [(1/t_{2\ closed}) \cdot f2]$ for mean opening rate and $(\tau_{1\ open} \cdot f_1) + (\tau_{2\ open} \cdot f_2)$ for mean open time, where $\tau_1$ and $\tau_2$ represent the fast and slow components of the open and closed time constants and $f_1$ and $f_2$ represent the fractional contribution of that particular component. Data used from Table II (filled symbols) and for another channel studied at 0, 50, and 100 μM DP4 (open symbols). Data trends in each panel were estimated by a sigmoidal fit based on a Boltzmann function. Same experimental conditions as in Fig. 11.

mM $Mg^{2+}$ solution (Fig. 10 A) is considerably greater than predicted by Scheme I using the parameter values given in legend to Fig. 9, whereas the suppression of spark frequency on increasing [$Mg^{2+}$] from 1.87 to 3.0 mM in the presence of 150 μM DP4 (Fig. 10 B) is more similar to that predicted by Scheme I using the values in Fig. 9. For these calculations and the simulations in Fig. 9, we assumed that a channel without DP4 bound was as likely to proceed to the open state as one with DP4 bound (i.e., $K_{D2} = K_{D2}^*$ and $k = k^*$). However, it may be possible that by decreasing the affinity of the A-site for $Mg^{2+}$ (i.e., making $K_{D2}^* > K_{D2}$) and/or increasing the affinity of the same site for $Ca^{2+}$ ($k^* > k$) when DP4 is bound, Scheme I might more closely account for the effect of DP4 in Fig. 10 while still reproducing the effects in Fig. 9.

*Effects of DP4 on Single Channels Isolated From Frog SR*

Single-channel current recordings (Fig. 11 A) demonstrate that addition of 50 μM DP4 to the cytoplasmic (cis) side of frog skeletal RyRs reconstituted in planar lipid bilayer induced a large increase in the channel open probability. In contrast, addition of 100 μM DP4mut (Fig. 11 B) in the same fashion did not produce any significant effect on channel open probability. The $Cs^+$ currents presented here show that the presence of DP4 or DP4mut at the channel did not produce an appreciable difference in the current amplitude compared with the currents recorded in the absence of either peptide (Fig. 11). In these bilayer experiments, $Mg^{2+}$-free solutions were used to increase the frequency of channel opening, $Cs^+$ was used as the current carrier so as to increase the channel current and, thus, improve detection of channel opening, and the cytosolic solution was pCa ~ 5 to activate channel opening by CICR.

*Concentration Dependence of DP4 Effects on Open Probability and Opening Rate of Single $Ca^{2+}$ Release Channels in Bilayers*

The concentration dependence of DP4 effects was also investigated using frog skeletal RyRs incorporated in lipid bilayers. The majority of these studies also were performed in $Mg^{2+}$-free solutions to increase channel opening, and thereby facilitate the acquisition of large numbers of channel openings for statistical analysis. $Cs^+$ was the current carrier and pCa ~ 5 was used to activate channel opening. Over the [DP4] range from 10 to 100 μM, increasing the DP4 concentration caused a saturating dose-dependent increase in the channel open probability (Fig. 12 A) with a calculated $EC_{50}$ of 4.4 μM and a maximum open probability of 0.82. This observed high apparent affinity of DP4 for the channels in a bilayer is in sharp contrast to the much lower apparent affinity indicated by the observed linearity of the increase in frequency of $Ca^{2+}$ sparks in muscle fibers with increasing



Downloaded from http://rupress.org/jgp/article-pdf/119/1/15/1216418/8439.pdf by guest on 16 May 2022

TABLE II

*Dwell-time Constants for RyRs Isolated from Frog Muscle at Different Cis DP4 Concentrations*

| | Closed time constants | | Open time constants | |
|---|---|---|---|---|
| [DP4] | Percent $\tau_1$ closed | Percent $\tau_2$ closed | Percent $\tau_1$ open | Percent $\tau_2$ open |
| *μM* | *ms* | *ms* | *ms* | *ms* |
| 0 | 1.89 (39) | 21.4 (61) | 0.81 (77) | 8.30 (23) |
| 10 | 1.10 (48) | 12.4 (52) | 0.88 (53) | 14.4 (47) |
| 30 | 0.95 (52) | 13.4 (48) | 0.87 (49) | 14.9 (51) |
| 50 | 0.85 (59) | 10.7 (41) | 0.90 (49) | 16.8 (51) |
| 100 | 0.80 (55) | 9.87 (45) | 0.94 (47) | 17.9 (53) |

Time constants from open and closed dwell-time histograms for frog $Ca^{2+}$ release channels (RyRs) treated with various concentrations of DP4. Symmetric solutions contained 300 mM cesium methanesulfonate and 10 mM Na-HEPES, pH 7.2, with no added $Mg^{2+}$ and pCa $\sim$ 5.

DP4 up to 300 μM, and may be related to the absence of $Mg^{2+}$ in the bilayer studies.

Open and closed dwell-time histograms were derived for the channels in the control condition as well as for the channels treated with the increasing concentrations of DP4. Data from each tested condition, including the control condition in the absence of DP4, could be best fit with two open and two closed time constants. The fact that RyR channels in bilayers exhibit two open and two closed states in the absence of both DP4 and $Mg^{2+}$ indicates that Scheme I will not successfully account for the bilayer data. Scheme I does not provide a sufficient number of states in the absence of both $Mg^{2+}$ and DP4 to account for two open and two closed time constants. Thus, the channel gating behavior in the bilayer experiments cannot be interpreted using Scheme I, even though Scheme I does provide a good general description of the effects of $Mg^{2+}$ and DP4 on the rate of occurrence of $Ca^{2+}$ sparks in muscle fibers.

Both of the closed time constants obtained from single-channel recordings of frog RyRs in bilayers decreased with increasing [DP4] (Table II). Using the closed time constants in Table II, we have calculated the mean opening rate of the channels in the presence and in the absence of DP4 using the equation in the Fig. 12 legend. As seen in Fig. 12 B, the mean opening rate of frog RyRs in bilayers increased with increasing concentrations of DP4. This increase in channel opening rate is analogous to the increase in $Ca^{2+}$ spark frequency detected in the presence of DP4 in the muscle fiber experiments. However, whereas spark frequency increased linearly with [DP4] (up to 300 μM) in muscle fibers (Fig. 5 A), the opening rate constant of single RyR channels in the bilayer saturated at [DP4] of $\sim$60 μM (Fig. 12 B). Thus, the apparent affinity of DP4 for frog RyRs obtained from the observed increase in single-channel opening rate in bilayers was again much higher than the apparent affinity of DP4 for frog RyRs based on the increase in frequency of $Ca^{2+}$ sparks observed in frog muscle fibers.

The difference in the apparent affinity of DP4 for the RyR in muscle fibers compared with bilayer experiments may be related to the relative availability of certain states of the channel in the two types of experiments. As described above, DP4 binding may require the channel to be in the conformation where the two domains that stabilize the closed state of the channel are only weakly interacting. To obtain reliable information regarding the kinetics of the channel, the bilayer experiments in Fig. 12 used a relatively high channel open probability, which was obtained under $Mg^{2+}$-free conditions that may destabilize the domain interactions and thus provide a more accessible binding site for the peptide. In contrast, the muscle fiber experiments require a very low channel opening probability and consequently used conditions that stabilize interdomain interactions, which do not provide the optimal conditions for the binding of the peptide.

To investigate the interaction of DP4 with single channels in the presence of $Mg^{2+}$, some bilayer experiments were performed after addition of 1mM $Mg^{2+}$ to the cis side of the bilayer. 1 mM $Mg^{2+}$ virtually eliminated all channel activity under control conditions in the absence of DP4 ($P_{open} < 0.001$; $n = 4$ channels). Subsequent addition of 100 μM DP4 in 1 mM $Mg^{2+}$ increased $P_{open}$, but only to 0.078 ± 0.015 ($n = 4$). In 1 mM $Mg^{2+}$ the rate of opening of channels in the bilayer increased from 0.3 $s^{-1}$ in control conditions to 9 $s^{-1}$ in 100 μM DP4. In contrast, in the absence of $Mg^{2+}$, at [DP4] of 50 μM the channel $P_{open}$ was near unity (Figs. 11 A and 12 A) and the rate of opening was $\sim$700 $s^{-1}$ (Fig. 12 B). We attempted to explore the DP4 affinity in bilayer experiments in 1 mM $Mg^{2+}$ using higher concentrations of DP4. Unfortunately the presence of DP4 at concentrations higher than 100 μM caused the bilayer to become unstable, so the concentration dependence of the effects of DP4 on channel opening rate in 1 mM $Mg^{2+}$ solution in bilayers could not be determined. However, our observations are not inconsistent with the possibility that in bilayer experiments DP4 may have a lower apparent affinity for RyR in the presence of 1 mM $Mg^{2+}$ than in $Mg^{2+}$-free conditions. In that case, $Mg^{2+}$ would modulate the ability of DP4 to unlock the channel in the bilayer experiments, which is analogous to the $Mg^{2+}$ effect on DP4 observed in the muscle fiber experiments (Figs. 7 and 8).

### *Effects of DP4 on Open Time of $Ca^{2+}$ Release Channels in Bilayers*

Channels treated with DP4 in the bilayer exhibited similar fast open time constants as the untreated channels at all [DP4], but the slow open time constants as well as the percent contribution of slow openings increased



Downloaded from http://rupress.org/jgp/article-pdf/119/1/15/1216418/8439.pdf by guest on 16 May 2022

with the increasing [DP4] (Table II). Because of the increase in the open-time constants, the mean open times of the channels also increased with [DP4] (Fig. 12 C). Although in muscle fibers we observed small but statistically significant differences in $Ca^{2+}$ spark properties between events detected in absence and in the presence of DP4, the magnitude of these changes was extremely small when compared with the changes in channel open time in the bilayer experiments. Currently, we cannot explain why, in the presence of DP4, the apparent channel open time was relatively unaltered in the muscle fibers (Fig. 5, B and C), whereas the mean open time of the single channels in the bilayers increased with [DP4] (Fig. 12 C).

One possibility that might account for the observed increase in channel open time in bilayers in the presence of DP4, but the lack of effect of DP4 on spark properties in muscle fibers is that the bilayer experiments in Fig. 12 were conducted in absence of $Mg^{2+}$. However, the absence of $Mg^{2+}$ does not appear to explain this difference. In 1 mM $Mg^{2+}$, in the absence of DP4 there were barely any detectable openings in the bilayer experiments, but the few that occurred were all of brief (<1 ms) duration. In contrast, in the presence of DP4 (100 μM), we obtained two mean open times, $\tau_1$ = 0.5, 0.3, and 0.5 and $\tau_2$ = 1.5, 2.3, and 1.9 ms (three channels), in 1 mM $Mg^{2+}$, indicating that DP4 increases the open time of single frog RyRs in bilayers even in the presence of 1 mM $Mg^{2+}$. Thus, DP4 appears to increase channel open time in the bilayers but not in the muscle fibers, possibly indicating differences in channel closing mechanisms terminating $Ca^{2+}$ sparks in muscle fibers compared with single channels in the bilayer. The channel open time in the presence of 1 mM $Mg^{2+}$ and 100 μM DP4 in the bilayer experiments was considerably shorter than the mean spark rise time of ~5 ms in the muscle fiber experiments (Fig. 3 B). Thus, either the individual channel openings are longer under the conditions of the muscle fiber experiments than in the bilayer studies, or multiple channel openings and closings may occur during the rising phase of a single $Ca^{2+}$ spark.

## DISCUSSION

This report describes the effects of the DP4 peptide on local SR $Ca^{2+}$ release events ($Ca^{2+}$ sparks) detected by laser scanning confocal microscopy, in permeabilized, cut frog skeletal muscle fibers, as well as the effects of DP4 on frog SR vesicles and on frog single RyR $Ca^{2+}$ release channels reconstituted in planar lipid bilayers. DP4 duplicates the amino acid sequence of the central domain of the RyR1 that contains a mutation site for MH. It appears that the primary amino acid sequence in this region of RyR is highly conserved. Rabbit RyR1 and frog RyRα sequences are identical within this region of the channel, and there was more then 90% identity between RyR1 and RyRβ as well. Interaction of DP4 with the channel potentially interferes with the normal intrachannel domain–domain interaction that may play a key role in stabilizing one of the closed states of the channel (Yamamoto et al., 2000). Our results demonstrate that DP4 increases the frequency of occurrence of $Ca^{2+}$ sparks without appreciably altering the properties of the individual $Ca^{2+}$ sparks. We also find that DP4 increases the channel open probability of frog skeletal RyRs in bilayers and increases the [$^3$H]ryanodine binding to vesicles isolated from frog skeletal muscle. In contrast, application of 50 μM of DP4mut, a peptide identical to DP4 except for an $Arg^{17}$ to $Cys^{17}$ mutation identical to that found in MH, had no appreciable effect on $Ca^{2+}$ spark frequency (Figs. 1–3). These results suggest that DP4 increases $Ca^{2+}$ release by stabilizing the RyRs in a conformation in which the affected channels are more susceptible to activation by $Ca^{2+}$ (CICR).

### *Effects of DP4 on Opening and Closing of $Ca^{2+}$ Channels*

In muscle fiber experiments, DP4 increased the frequency of occurrence of $Ca^{2+}$ sparks, indicating that DP4 increased the rate of opening of the channels responsible for initiating $Ca^{2+}$ sparks. In bilayer experiments, DP4 also caused an analogous increase in channel opening rate and channel open probability. The data from the bilayer experiments also indicate that application of increasing concentrations of DP4 promoted a dose-dependent increase in the channel mean open time (Fig. 7 C). However, in the muscle fiber experiments the DP4 did not alter the spark rise time. The spark rise time corresponds to the total time interval during which the channel or channels generating the spark are open (Lacampagne et al., 1999). Thus, DP4 did not influence the overall time period during which the channels generating a spark were open in the muscle fiber experiments. In the muscle fibers, the spark rise time might encompass multiple brief openings of one or more channels (Schneider, 1999). In that case, the individual channel openings could conceivably be prolonged, giving rise to an increase in the total summed duration of all openings, whereas the time interval encompassing all such openings could still remain unchanged, giving an unaltered spark rise time. However, an increase in such individual open times would still be expected to cause an increase in the total amount of $Ca^{2+}$ released, and consequently an increase in spark amplitude, which was not observed. Thus, it seems highly unlikely that DP4 increases channel open time in the muscle fibers as it does with single channels in the bilayer. The channel activity underlying the $Ca^{2+}$ sparks in muscle fibers consequently appears to terminate by a mechanism independent of DP4, whereas single-channel openings in the bilayer are prolonged by DP4.



Downloaded from http://rupress.org/jgp/article-pdf/119/1/15/1216418/8439.pdf by guest on 16 May 2022

The observation that DP4 increases the open time of channels in bilayers but not in muscle fibers suggests that there are different regulatory mechanisms governing channel open time in the functionally intact muscle fibers, where channels and other components may interact, compared with the isolated single channels in the bilayer. Furthermore, the basic mechanism of channel closing, which determines channel open time, may be different in functioning muscle fibers compared with single channels in bilayers. In the muscle fibers, $Ca^{2+}$ is the current carrier and the channels are likely to close by a $Ca^{2+}$-dependent inactivation mechanism generated by high local [$Ca^{2+}$] in the immediate vicinity of the open channel, basically an irreversible step driven by the $Ca^{2+}$ gradient across the SR membrane. In contrast, in the bilayer studies, $Cs^{+}$ was the current carrier and channel closure presumably occurred by simple reversal of channel opening, and not by inactivation.

We have previously reported that application of another synthetic peptide ($IpTx_a$) induced long duration subconductance openings of the RyR in both skeletal muscle and in bilayer preparations (Shtifman et al., 2000). According to those data, regardless of the experimental preparations, $IpTx_a$ locked the channel in a specific, very long-lasting open substate. Thus, the binding of $IpTx_a$ overrides the normal closing mechanism of RyRs in both the muscle fibers and in bilayers. In contrast, in muscle fibers, DP4 does not appear to have such overriding effect on the open channel. Our results demonstrate that DP4 affects the RyRs in muscle fibers in their closed state by increasing their opening rate, but it appears that DP4 does not override the channel closing mechanism in muscle fibers.

In principle, DP4 might promote channel opening by transiently stabilizing the RyRs in a conformation where the $NH_2$-terminal and central domains either do not interact or interact more weakly than in the absence of DP4. There are at least two potential mechanisms by which DP4 could interact with the channel. One possibility is that DP4 could directly bind to one of the domains and effectively displace the other. Another possibility is that RyRs could spontaneously isomerize or alternate between two distinctly different, closed conformations. In one of the conformations, the two domains within the channel would interact tightly and in the other conformation, this interaction may be weakened or may be absent. It is possible that DP4 could preferentially interact with the channel when the domain–domain interaction is weakened. Preferential interaction of DP4 with channels with weakened interdomain interaction would be consistent with the much higher apparent affinity of DP4 for the channel in the present bilayer experiments compared with the present muscle fiber experiments. At this point, we cannot definitively determine which mechanism is used by the DP4. However, regardless of how this peptide interferes with the interdomain interaction, it appears that after binding to the channel, DP4 transiently stabilizes the two domains in the conformation that predisposes the channels for activation.

### *$Mg^{2+}$ Inhibition of $Ca^{2+}$ Release*

Results presented in this study provide further evidence for intimate involvement of myoplasmic $Mg^{2+}$ in the regulation of $Ca^{2+}$ release from the SR in muscle fibers. The results of the fit in Fig. 8 A gave a value $n = 1.64$, in close agreement with 1.6 determined by Lacampagne et al. (1998). Thus, in the absence of DP4, at least two $Mg^{2+}$ binding sites must be freed of $Mg^{2+}$ to remove the inhibitory effect of $Mg^{2+}$ on the opening of the SR $Ca^{2+}$ release channel initiating a $Ca^{2+}$ spark. According to the data shown in Fig. 7, $Mg^{2+}$ also plays an important role in modulation of the DP4 effect. It seems that at lower myoplasmic [$Mg^{2+}$], DP4 is more effective at eliciting $Ca^{2+}$ sparks than at higher [$Mg^{2+}$] (Fig. 8 B). As mentioned earlier the effectiveness of DP4 in enhancing channel opening is represented by the magnitude of the slope of the graph of spark rate versus [DP4] at each [$Mg^{2+}$] (Figs. 6 and 8 B). Since DP4 was more effective in eliciting the increase in $Ca^{2+}$ spark frequency at lower [$Mg^{2+}$] (Figs. 7 and 8 B), we conclude that magnesium plays an intimate role in modulation of the effectiveness of DP4, and perhaps even in regulation of the interdomain interactions. Interestingly, results of the fit in Fig. 8 B, gave a value for n equal to 0.89, suggesting that there may be only a single $Mg^{2+}$ binding site involved in regulation of effectiveness of DP4. We speculate that the single $Mg^{2+}$ binding site controlling the increase in effectiveness of DP4 at lower myoplasmic [$Mg^{2+}$] was the low affinity, I-binding site for $Mg^{2+}$.

### *Reaction Scheme and Molecular Model for $Ca^{2+}$ Spark Activation with and without DP4*

Based on the above considerations and our current results we proposed a kinetic reaction scheme (Scheme I), and the following corresponding molecular model (Fig. 13) for action of DP4 in muscle fibers. Our reaction scheme is modified from a scheme for $Ca^{2+}$ spark activation due to lowered [$Mg^{2+}$] proposed previously (Lacampagne et al., 1998; Scheme I). Each RyR should have two divalent cation binding sites (Laver et al., 1997b; Meissner et al., 1997), the high affinity, A-site, with bound $Ca^{2+}$ ion depicted in red and $Mg^{2+}$ depicted in green, and the low affinity, I-site, with bound $Mg^{2+}$ ion depicted in green (Scheme I and Fig. 13). In addition to the ion binding sites, the channel may have several domains that interact with each other. We predict that interaction of these domains stabilizes the channel in a closed conformation (Fig. 13, top left), and that



Downloaded from http://rupress.org/jgp/article-pdf/119/1/15/1216418/8439.pdf by guest on 16 May 2022

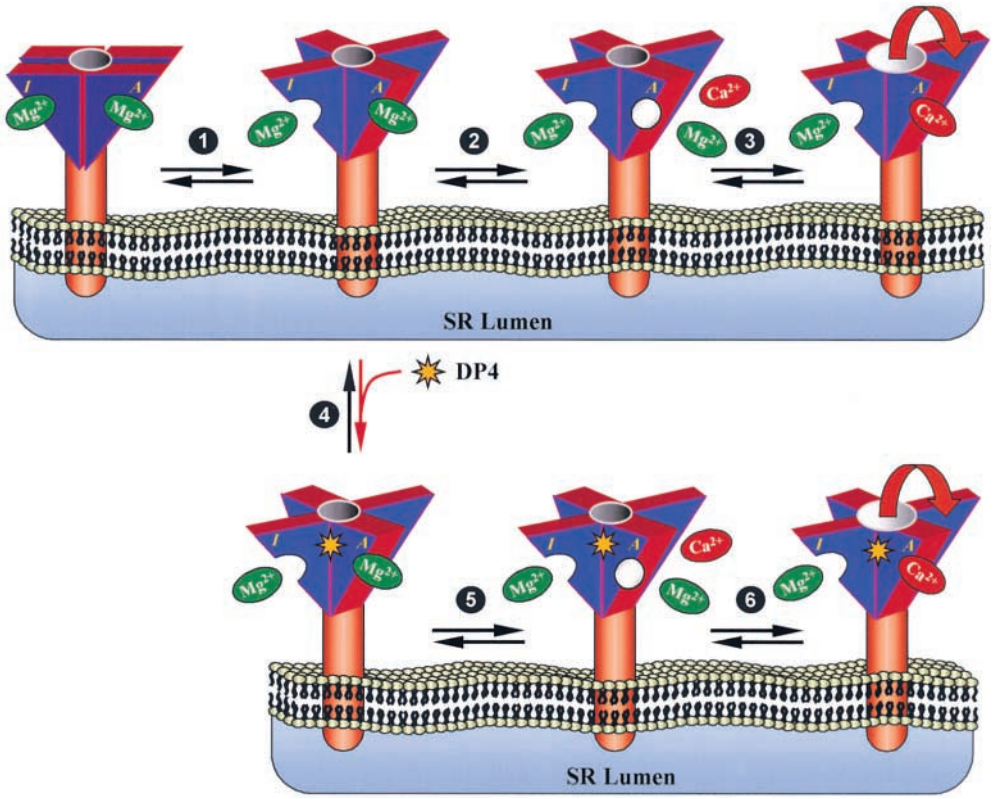


FIGURE 13. Cartoon representation of possible DP4 mechanism. A RyR $Ca^{2+}$ release channel at rest has both divalent cation sites (high affinity [A] and low affinity [I]) occupied by $Mg^{2+}$ (green), with the appropriate domains interacting. For DP4 to bind to the appropriate region of the RyR, the interaction of the involved domains should be disrupted or weakened. Loosening of the interdomain interactions causes the channel to undergo a large conformational change, which is either facilitated or accompanied by dissociation of $Mg^{2+}$ from the I-site (step 1). Binding of DP4 (step 4, red arrow) should temporarily stabilize the noninteracting conformation of the channel and perhaps promotes $Mg^{2+}$ dissociation from the A-site (step 5), which would allow for $Ca^{2+}$ (red) to bind to the A-site and activate $Ca^{2+}$ release form the channel (step 6). Note, binding of DP4 forces the equilibrium to the right as indicated by the red arrow. In the absence of DP4, the first step in the initiation of $Ca^{2+}$ release involves dissociation of $Mg^{2+}$ from the I-site, accompanied by disruption of the interdomain interaction (step 1). Next steps, involve dissociation of $Mg^{2+}$ from the high affinity binding site (step 2) and activation of $Ca^{2+}$ release (step 3). Note, since spontaneous channel opening in resting fibers is infrequent under the conditions of our experiments, the majority of the channels do not go through step 6.

when this interaction is disrupted (Fig. 13, step 1) the channel will be predisposed for activation. A channel at rest, in the cytosolic environment of submicromolar $Ca^{2+}$ and millimolar $Mg^{2+}$, will have both divalent cation sites occupied by $Mg^{2+}$, and be in the conformation with domains interacting. We hypothesize that for DP4 to bind to the appropriate region of the RyR, the interaction of the involved domains should be disrupted or weakened. Since DP4 binding to the channel is modulated by $Mg^{2+}$, presumably at the low affinity binding site, we predict that the loosened domain–domain interaction is either facilitated or accompanied by dissociation of $Mg^{2+}$ from the I-site (Fig. 13, step 1). It is likely that there would be some type of equilibrium between the interacting and noninteracting conformation of the channel. However, since magnesium concentrations used here, in our muscle fiber experiments were typically above the predicted $K_d$ (Ogawa et al., 2000), the channel should be predominantly in the conformation where two domains interact with each other. This would explain why, under physiological conditions, the $Ca^{2+}$ spark frequency in our fibers is extremely low. Binding of DP4 (Fig. 13, step 4) should temporarily stabilize the noninteracting conformation of the channel, promoting $Mg^{2+}$ dissociation from the A-site (Fig. 13, step 5) and $Ca^{2+}$ binding to the A-site (Fig. 13, step 6), thereby activating $Ca^{2+}$ release form the channel.

In the absence of DP4, spontaneous $Ca^{2+}$ release events from the SR are generated by a mechanism similar to the one described above. Once again, the first step in the initiation of $Ca^{2+}$ release would involve dissociation of $Mg^{2+}$ from the I-site accompanied by disruption of the interdomain interaction (Fig. 13, step 1). Next (Fig. 13, step 2), instead of binding DP4, $Mg^{2+}$ at the A-site should dissociate either spontaneously or with the help of other modulators of the RyRs, such as adenine nucleotides or calmodulin (Zucchi and Ronca-Testoni, 1997). Step 3 (Fig. 13) involves binding of



Downloaded from http://rupress.org/jgp/article-pdf/119/1/15/1216418/8439.pdf by guest on 16 May 2022

$Ca^{2+}$ to its high affinity binding site and activation of $Ca^{2+}$ release.

### *$Ca^{2+}$ Release in MH*

Since DP4 produces a pseudo-MH condition it is instructive to look at the $Mg^{2+}$ inhibition of MHS channels. A report by Mickelson et al. (1990) has demonstrated that $Mg^{2+}$ is a less effective inhibitor of [$^3$H]ryanodine binding to MHS compared with the normal SR. These conclusions also are supported by investigations by Laver et al. (1997b) and Owen et al. (1997), which have shown that $Mg^{2+}$ is less effective at inhibiting MHS RyR1 channel opening as well as $Ca^{2+}$ release in mechanically peeled MHS muscle fibers, respectively. More recent investigations by Balog et al. (2001) have demonstrated that MHS channels that carry the porcine $Arg^{615}$ to $Cys^{615}$ mutation display a reduced affinity for $Ca^{2+}$ and $Mg^{2+}$ at the I-site compared with the normal RyR1. They also have shown that the A-site of the MHS RyR1 has a lower affinity for $Mg^{2+}$ and a higher affinity for $Ca^{2+}$ compared with the wild-type channels.

In summary, we have investigated the effects of DP4 on local $Ca^{2+}$ release in frog skeletal muscle fibers and on RyRs reconstituted in planar lipid bilayers. We found that DP4 elicits an increase in $Ca^{2+}$ release by interfering with a domain–domain interaction within the RyRs. The disrupted interdomain interaction facilitates removal of $Mg^{2+}$ inhibition from the channels and may be a key factor in activation of $Ca^{2+}$ release from the SR.

This work was supported by research grants from the National Institutes of Health (R01-NS23346 to M.F. Schneider, F32-AR08544 to C.W. Ward, R01-AR16922 to N. Ikemoto, and PO1 HL47053 to H.H. Valdivia). H.H. Valdivia is a recipient of an Established Investigator Award from the American Heart Association.

*Submitted: 14 May 2001*
*Revised: 9 November 2001*
*Accepted: 14 November 2001*

## REFERENCES

Balog, E.M., B.R. Fruen, N.H. Shomer, and C.F. Louis. 2001. Divergent effects of the malignant hyperthermia-susceptible arg(615)→cys mutation on the $Ca^{2+}$ and $Mg^{2+}$ dependence of the RyR1. *Biophys. J.* 81:2050–2058.

Chen, S.R., and D.H. MacLennan. 1994. Identification of calmodulin, $Ca^{2+}$, and ruthenium red-binding domains in the $Ca^{2+}$ release channel (ryanodine receptor) of rabbit skeletal muscle sarcoplasmic reticulum. *J. Biol. Chem.* 269:22698–22704.

Cheng, H., L.S. Song, N. Shirokova, A. Gonzalez, E.G. Lakatta, E. Rios, and M.D. Stern. 1999. Amplitude distribution of calcium sparks in confocal images: theory and studies with an automatic detection method. *Biophys. J.* 76:606–617.

El-Hayek, R., M. Yano, and N. Ikemoto. 1995. A conformational change in the junctional foot protein is involved in the regulation of Ca $^{2+}$ release from sarcoplasmic reticulum. Studies on polylysine-induced $Ca^{2+}$ release. *J. Biol. Chem.* 270:15634–15638.

El-Hayek, R., Y. Saiki, T. Yamamoto, and N. Ikemoto. 1999. A postulated role of the near amino-terminal domain of the ryanodine receptor in the regulation of the sarcoplasmic reticulum $Ca^{2+}$ channel. *J. Biol. Chem.* 274:33341–33347.

Fill, M., E. Stefani, and T.E. Nelson. 1991. Abnormal human sarcoplasmic reticulum $Ca^{2+}$ release channels in malignant hyperthermic skeletal muscle. *Biophys. J.* 59:1085–1090.

Inui, M., A. Saito, and S. Fleischer. 1987. Isolation of the ryanodine receptor from cardiac sarcoplasmic reticulum and identity with the feet structures. *J. Biol. Chem.* 262:15637–15642.

Jayaraman, T., A.M. Brillantes, A.P. Timerman, S. Fleischer, H. Erdjument-Bromage, P. Tempst, and A.R. Marks. 1992. FK506 binding protein associated with the calcium release channel (ryanodine receptor). *J. Biol. Chem.* 267:9474–9477.

Klein, M.G., H. Cheng, L.F. Santana, Y.-H. Jiang, W.J. Lederer, and M.F. Schneider. 1996. Two mechanisms of quantized calcium release in skeletal muscle. *Nature.* 379:455–458.

Lacampagne, A., M.G. Klein, and M.F. Schneider. 1998. Modulation of the frequency of spontaneous sarcoplasmic reticulum $Ca^{2+}$ release events ($Ca^{2+}$ sparks) by myoplasmic [$Mg^{2+}$] in frog skeletal muscle. *J. Gen. Physiol.* 111:207–224.

Lacampagne, A., C.W. Ward, M.G. Klein, and M.F. Schneider. 1999. Time course of individual $Ca^{2+}$ sparks in frog skeletal muscle recorded at high time resolution. *J. Gen. Physiol.* 113:187–198.

Lamb, G.D., and D.G. Stephenson. 1991. Effect of $Mg^{2+}$ on the control of $Ca^{2+}$ release in skeletal muscle fibres of the toad. *J. Physiol.* 434:507–528.

Lamb, G.D., M.A. Cellini, and D.G. Stephenson. 2001. Different $Ca^{2+}$ releasing action of caffeine and depolarisation in skeletal muscle fibres of the rat. *J. Physiol.* 531:715–728.

Laver, D.R., T.M. Baynes, and A.F. Dulhunty. 1997a. Magnesium inhibition of ryanodine-receptor calcium channels: evidence for two independent mechanisms. *J. Membr. Biol.* 156:213–229.

Laver, D.R., V.J. Owen, P.R. Junankar, N.L. Taske, A.F. Dulhunty, and G.D. Lamb. 1997b. Reduced inhibitory effect of $Mg^{2+}$ on ryanodine receptor-$Ca^{2+}$ release channels in malignant hyperthermia. *Biophys. J.* 73:1913–1924.

Meissner, G. 1994. Ryanodine receptor/$Ca^{2+}$ release channels and their regulation by endogenous effectors. *Annu. Rev. Physiol.* 56: 485–508.

Meissner, G., E. Rios, A. Tripathy, and D.A. Pasek. 1997. Regulation of skeletal muscle $Ca^{2+}$ release channel (ryanodine receptor) by $Ca^{2+}$ and monovalent cations and anions. *J. Biol. Chem.* 272:1628–1638.

Melzer, W., A. Herrmann-Frank, and H.C. Lüttgau. 1995. The role of $Ca^{2+}$ ions in excitation-contraction coupling of skeletal muscle fibres. *Biochim. Biophys. Acta.* 1241:59–116.

Mickelson, J.R., and C.F. Louis. 1996. Malignant hyperthermia: excitation-contraction coupling, $Ca^{2+}$ release channel, and cell $Ca^{2+}$ regulation defects. *Physiol. Rev.* 76:537–592.

Mickelson, J.R., E.M. Gallant, L.A. Litterer, K.M. Johnson, W.E. Rempel, and C.F. Louis. 1988. Abnormal sarcoplasmic reticulum ryanodine receptor in malignant hyperthermia. *J. Biol. Chem.* 263:9310–9315.

Mickelson, J.R., L.A. Litterer, B.A. Jacobson, and C.F. Louis. 1990. Stimulation and inhibition of [$^3$H]ryanodine binding to sarcoplasmic reticulum from malignant hyperthermia susceptible pigs. *Arch. Biochem. Biophys.* 278:251–257.

Nakai, J., T. Tanabe, T. Konno, B. Adams, and K.G. Beam. 1998. Localization in the II-III loop of the dihydropyridine receptor of a sequence critical for excitation-contraction coupling. *J. Biol. Chem.* 273:24983–24986.

Ogawa, Y., N. Kurebayashi, and T. Murayama. 2000. Putative roles of type 3 ryanodine receptor isoforms (RyR3). *Trends Cardiovasc. Med.* 10:65–70.

Ohta, T., M. Endo, T. Nakano, Y. Morohoshi, K. Wanikawa, and A. Ohga. 1989. $Ca^{2+}$-induced $Ca^{2+}$ release in malignant hyperthermia-susceptible pig skeletal muscle. *Am. J. Physiol.* 256:C358–C367.

Owen, V.J., N.L. Taske, and G.D. Lamb. 1997. Reduced $Mg^{2+}$ inhi-



Downloaded from http://rupress.org/jgp/article-pdf/119/1/15/1216418/8439.pdf by guest on 16 May 2022

bition of $Ca^{2+}$ release in muscle fibers of pigs susceptible to malignant hyperthermia. *Am. J. Physiol.* 272:C203–C211.

Schneider, M.F. 1994. Control of calcium release in functioning skeletal muscle fibers. *Annu. Rev. Physiol.* 56:463–484.

Schneider, M.F. 1999. $Ca^{2+}$ sparks in frog skeletal muscle: generation by one, some, or many SR $Ca^{2+}$ release channels? *J. Gen. Physiol.* 113:365–372.

Schneider, M.F., and M.G. Klein. 1996. Sarcoplasmic calcium sparks activated by fiber depolarization and by cytosolic $Ca^{2+}$ in skeletal muscle. *Cell Calcium.* 20:123–128.

Serysheva, I.I., M. Schatz, M. van Heel, and S.L. Hamilton. 1999. Structure of the skeletal muscle calcium release channel activated with $Ca^{2+}$ and AMP-PCP. *Biophys. J.* 77:1936–1944.

Sharma, M.R., L.H. Jeyakumar, S. Fleischer, and T. Wagenknecht. 2000. Three-dimensional structure of ryanodine receptor isoform three in two conformational states as visualized by cryo-electron microscopy. *J. Biol. Chem.* 275:9485–9491.

Shomer, N.H., C.F. Louis, M. Fill, L.A. Litterer, and J.R. Mickelson. 1993. Reconstitution of abnormalities in the malignant hyperthermia-susceptible pig ryanodine receptor. *Am. J. Physiol.* 264: C125–C135.

Shomer, N.H., J.R. Mickelson, and C.F. Louis. 1994. Ion selectivity of porcine skeletal muscle $Ca^{2+}$ release channels is unaffected by the $Arg^{615}$ to $Cys^{615}$ mutation. *Biophys. J.* 67:641–646.

Shtifman, A., C.W. Ward, J. Wang, H.H. Valdivia, and M.F. Schneider. 2000. Effects of imperatoxin A on local sarcoplasmic reticulum $Ca^{2+}$ release in frog skeletal muscle. *Biophys. J.* 79:814–827.

Takeshima, H., S. Nishimura, T. Matsumoto, H. Ishid, K. Kangaw, N. Minamin, H. Matsu, M. Ued, M. Hanaok, and T. Hiros. 1989. Primary structure and expression from complementary DNA of skeletal muscle ryanodine receptor. *Nature.* 339:439–445.

Tanabe, T., K.G. Beam, B.A. Adams, T. Niidome, and S. Numa. 1990. Regions of the skeletal muscle dihydropyridine receptor critical for excitation-contraction coupling. *Nature.* 346:567–569.

Timerman, A.P., E. Ogunbumni, E. Freund, G. Wiederrecht, A.R. Marks, and S. Fleischer. 1993. The calcium release channel of sarcoplasmic reticulum is modulated by FK-506-binding protein. Dissociation and reconstitution of FKBP-12 to the calcium release channel of skeletal muscle sarcoplasmic reticulum. *J. Biol. Chem.* 268:22992–22999.

Tsuchiya, T. 1988. Passive interaction between sliding filaments in the osmotically compressed skinned muscle fibers of the frog. *Biophys. J.* 53:415–423.

Ward, C.W., A. Lacampagne, M.G. Klein, and M.F. Schneider. 1998. $Ca^{2+}$ spark properties in saponin permeabilized skeletal muscle. *Byophys. J.* 72:A269. (Abstr.)

Yamamoto, T., R. El-Hayek, and N. Ikemoto. 2000. Postulated role of interdomain interaction within the ryanodine receptor in $Ca^{2+}$ channel regulation. *J. Biol. Chem.* 275:11618–11625.

Zucchi, R., and S. Ronca-Testoni. 1997. The sarcoplasmic reticulum $Ca^{2+}$ channel/ryanodine receptor: modulation by endogenous effectors, drugs and disease states. *Pharmacol. Rev.* 49:1–51.

Downloaded from http://rupress.org/jgp/article-pdf/119/1/15/1216418/8439.pdf by guest on 16 May 2022